Progress In Electromagnetics Research, PIER 44, 231–248, 2004

WIDE-ANGLE RADAR TARGET RECOGNITION WITH SUBCLASS CONCEPT

D.-K. Seo

Electrical and Computer Engineering Division
Pohang University of Science and Technology
San 31 Hyoja-dong, Nam-gu, Pohang, Kyungbuk, 790-784, Korea

K. T. Kim

Department of Electrical Engineering and Computer Science
Yeungnam University
213-1, Daedong, Kyongsan, Kyungbuk, 712-749, Korea

I.-S. Choi and H.-T. Kim

Electrical and Computer Engineering Division
Pohang University of Science and Technology
San 31 Hyoja-dong, Nam-gu, Pohang, Kyungbuk, 790-784, Korea

Abstract—The range profile is an easily obtainable and promising feature vector for a real-time radar target recognition system. However, the range profile is highly dependent on the aspect angle of a target. This dependency makes the recognition over a wide angular region difficult. In this paper, we propose a classifier with a subclass concept in order to solve this dependency problem. Recognition results with six aircraft models measured at a compact range facility are presented to show the effectiveness of the proposed classifier over a wide-angular region.

1. INTRODUCTION

Radar target recognition is a very difficult task, since the radar signature scattered from a target is very complex – it depends on the target geometry, the measured frequency, the aspect angle, and so on. Many different methods are used to extract the feature vector from the raw signal received by radar, such as the one-dimensional (1-D) range profile, the two-dimensional (2-D) synthetic aperture radar (SAR) or inverse synthetic aperture radar (SAR) image, natural frequency, and time-frequency analysis. Among these methods, natural frequency is based on the resonance phenomenon due to the specific target geometry. However, these methods require a pulsed radar system with a high signal-to-noise ratio (SNR) and a considerably short pulse, because the resonance phenomenon shows up in the late-time region of the time domain response. In other words, resonance appears behind the target response in the time-domain response and this late-time signal has a lower signal level than the signal from the target response. In the case of 2-D imagery (2-D SAR or ISAR image), a long waiting time is required to gather the data over many aspect angles. Furthermore, 2-D imagery needs a special motion compensation processing technique in order to compensate for the undesired motion of a target or a radar, such as yawing, rolling, pitch, acceleration, and etc. The time-frequency analysis shows the scattering points distribution as well as the frequency response. However, as in 2-D ISAR or SAR imagery, it is necessary to process two-dimensional data. However, in the actual battlefield, the received radar signal is very noisy and contaminated with clutter. Furthermore, for a rapid reaction pertinent to the battle situation, a target recognition system is required to process the data in real-time. For these reasons, the range profile is a very promising feature vector for a real-time radar target recognition system [1–3]. Also, if enough resolution is provided,

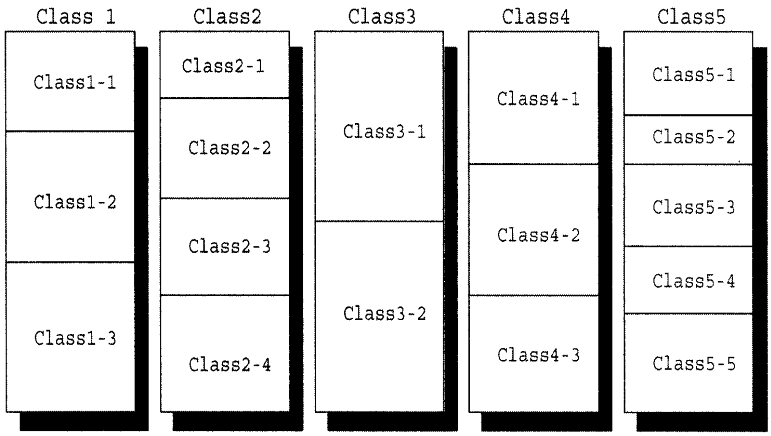

Figure 1. Division of each class with subclass concept.

the recognition results using the range profile may even be superior to recognition using the 2-D image [4].

The range profile shows radar cross section (RCS) distribution along the slant range direction of radar. In other words, the range profile is the time domain response of the scattering wave from a target. Therefore, the range profile is not easily contaminated by noise relative to the natural frequency. Furthermore, the range profile requires a very short time to acquire the data from radar and to process the raw data to the range profile, relative to 2-D imagery (SAR or ISAR imagery) or the time-frequency analysis.

However, radar target recognition using the range profile over the wide-angular region has one disadvantage; it considerably varies with the observation angle. If the observation angular region is wide and the feature vectors are post-processed from the range profile through a feature extraction technique, the feature vectors obtained from only one target occupy very scattered points in the feature space. If feature vectors from each class are scattered, the areas where the feature vectors from different classes are mixed become wide, and these areas make the classification task more difficult. As a result, the classification performance is degraded. In this paper, we propose a classifier with a subclass concept for radar target recognition using the range profile. The subclass concept means that each class is divided into several subclasses, such as in Fig. 1. In this paper, we use the clustering algorithm to divide each class into subclasses, after which the classifier is trained using the subclasses. The number of subclasses for each target is determined through an optimization with an appropriate cost function. These subdivided classes (subclasses) can reduce performance degradation due to the scattered feature vectors.

The remainder of this paper is organized as follows. In Section 2, we summarize a feature vector extraction technique in [1], which we use to post-process range profiles. In Section 3, we explain the subclass concept and the structures of the classifier with the subclass concept. Next, we present the integer-coded genetic algorithm (GA) for the selection of the number of subclasses. Finally, we demonstrate the performance of the classifier with the subclass concept. Experimental results using six aircraft models measured at the Pohang Science and Technology (POSTECH) compact range facility are presented. We compare the performance of the proposed classifier with that of the simple statistical classifier.

2. THE FEATURE VECTOR EXTRACTION TECHNIQUE USING CENTRAL MOMENTS AND PRINCIPAL COMPONENT ANALYSIS

In [1, 2], Kim et al. used the central moments, some mappings, and PCA to extract the efficient feature vectors, which have the characteristics of translation and level invariance, and small size from range profiles. The procedure of the scheme is as follows:

1. The calculation of central moments
2. The feature space mapping
3. The feature extraction using PCA

2.1. The Calculation of Central Moments

Central moments have the advantage that they guarantee translation and scale (level) invariance, enabling us to obtain a feature which is invariant with the distance between a radar and a target. After we acquire the range profiles of a target using inverse fast Fourier transform (IFFT) or high-resolution techniques, such as multiple signal classification (MUSIC) [5], we can obtain the p-th order central moments by the following equation,

$$\mu_p = \sum_{i=1}^{N_r} \left(\frac{r_i - \eta_r}{R_u}\right)^p \left[\frac{\bar{p}_m(r_i)}{\sum_{i=1}^{N_r} \bar{p}_m(r_i)}\right], \qquad r_i \in [0, R_u] \tag{1}$$

where

$$\eta_p = \sum_{i=1}^{N_r} r_i \left[\frac{\bar{p}_m(r_i)}{\sum_{i=1}^{N_r} \bar{p}_m(r_i)}\right], \tag{2}$$

$\bar{p}_m(r_i)$ is the normalized range profile, N_r is the number of range bin samplings, and R_u is the maximum unambiguous range. In this equation, $\left(\frac{r_i-\eta_r}{R_u}\right)$ is modified from $(r_i - \eta_r)$ to prevent the magnitude of moments from growing exponentially with increasing order p.

2.2. Feature Space Mapping

Using central moments in (1), the feature vector $\boldsymbol{f}$ can be represented as

$$\boldsymbol{f} = [f_1, f_2, \ldots, f_{p_{max}}]^T = [\mu_1, \mu_2, \ldots, \mu_{p_{max}}]^T \tag{3}$$

where p_{max} is the maximum order of central moments.

To train a classifier, it is necessary to construct a training database containing the feature vectors of many target classes and aspect angles. For N_c target classes and N_a aspects used for training, we can obtain the training database $\boldsymbol{F}$ using (3) as follows:

$$\begin{aligned}\boldsymbol{F} &= [\boldsymbol{f}_1 \ \boldsymbol{f}_2 \ \cdots \boldsymbol{f}_M] \\ &= \begin{bmatrix} f_{1,1} & f_{1,2} & \cdots & f_{1,M} \\ f_{2,1} & f_{2,2} & \cdots & f_{2,M} \\ \vdots & \vdots & \ddots & \vdots \\ f_{p_{max},1} & f_{p_{max},2} & \cdots & f_{p_{max},M} \end{bmatrix}\end{aligned} \tag{4}$$

where $M = N_a \times N_c$ and $\boldsymbol{F}$ is a $p_{max} \times M$ matrix.

In (4), in order for each column to provide equal weight in each dimension of the feature space, we normalize each column of $\boldsymbol{F}$ as follows:

$$\bar{f}_{ij} = \frac{f_{ij} - f_{i,min}}{f_{i,max} - f_{i,min}}, \quad i = 1, 2, \ldots, p_{max}, \ j = 1, 2, \ldots, M \tag{5}$$

where

$$\begin{aligned} f_{i,min} &= \text{minimum } f_{ij}, \quad j = 1, 2, \ldots, M \text{ for a given } i \\ f_{i,max} &= \text{maximum } f_{ij}, \quad j = 1, 2, \ldots, M \text{ for a given } i \end{aligned}$$

and therefore the normalized training database $\bar{\boldsymbol{F}}$ is established as follows:

$$\bar{\boldsymbol{F}} = \begin{bmatrix} \bar{f}_{1,1} & \bar{f}_{1,2} & \cdots & \bar{f}_{1,M} \\ \bar{f}_{2,1} & \bar{f}_{2,2} & \cdots & \bar{f}_{2,M} \\ \vdots & \vdots & \ddots & \vdots \\ \bar{f}_{p_{max},1} & \bar{f}_{p_{max},2} & \cdots & \bar{f}_{p_{max},M} \end{bmatrix} \tag{6}$$

2.3. The Feature Extraction with PCA

In fact, the central moment features have more redundant information as the order p increases. Therefore, another feature extraction technique is needed to reduce redundancy and feature dimension. The PCA, called Karhunen-Loeve transform, is applied to extract the post-processed feature vector. The procedure of transform is as follows [6]:

1. estimate the covariance matrix $\boldsymbol{R}_{\bar{\boldsymbol{f}}\bar{\boldsymbol{f}}}$

$$\boldsymbol{R}_{\bar{\boldsymbol{f}}\bar{\boldsymbol{f}}} = \frac{1}{M-1}\sum_{k=1}^{M}\left(\bar{\boldsymbol{f}}_k - \bar{\boldsymbol{m}}_{\bar{\boldsymbol{f}}}\right)\left(\bar{\boldsymbol{f}}_k - \bar{\boldsymbol{m}}_{\bar{\boldsymbol{f}}}\right)^T \tag{7}$$

   where $\boldsymbol{F} = [\bar{\boldsymbol{f}}_1 \bar{\boldsymbol{f}}_2 \cdots \bar{\boldsymbol{f}}_M]$, $\boldsymbol{m}_{\bar{\boldsymbol{f}}} = \frac{1}{M}\sum_{k=1}^{M}\bar{\boldsymbol{f}}_k$ and T denote the transpose of a matrix.

2. eigendecompose the covariance matrix $\boldsymbol{R}_{\bar{\boldsymbol{f}}\bar{\boldsymbol{f}}}$

$$\boldsymbol{R}_{\bar{\boldsymbol{f}}\bar{\boldsymbol{f}}} = \boldsymbol{V}\boldsymbol{\Lambda}\boldsymbol{V}^T \tag{8}$$

   where $\boldsymbol{\Lambda}$ is the diagonal matrix whose diagonal elements are eigenvalues and $\boldsymbol{V}$ is the matrix whose columns are eigenvectors.

3. construct the transformation matrix $\boldsymbol{W}$

$$\boldsymbol{W} = [\boldsymbol{v}_1\ \boldsymbol{v}_2\ \cdots\ \boldsymbol{v}_k] \tag{9}$$

   where $k < p_{max}$ and $\boldsymbol{v}_1, \boldsymbol{v}_2, \ldots, \boldsymbol{v}_k$ are the eigenvectors corresponding to the largest k eigenvalues.

4. transform the training data and the test data into a new feature space of dimension k as follows:

$$\boldsymbol{x}_i = \boldsymbol{W}^T\bar{\boldsymbol{f}}_i, \qquad i = 1, 2, \ldots, M. \tag{10}$$

After this procedure, training database is transformed as follows:

$$\begin{aligned} \bar{\boldsymbol{F}}' &= [\boldsymbol{x}_1\ \boldsymbol{x}_2\ \cdots \boldsymbol{x}_M] \\ &= \begin{bmatrix} x_{1,1} & x_{1,2} & \cdots & x_{1,M} \\ x_{2,1} & x_{2,2} & \cdots & x_{2,M} \\ \vdots & \vdots & \ddots & \vdots \\ x_{k,1} & x_{k,2} & \cdots & x_{k,M} \end{bmatrix} \end{aligned} \tag{11}$$

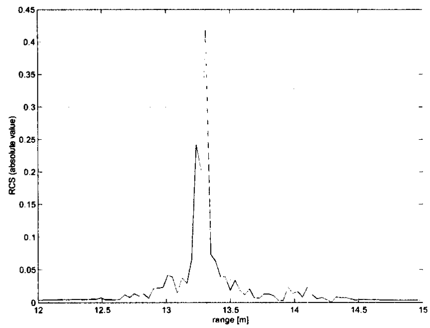

(a) The range profile of target-1 at the aspect angle of 0 deg.

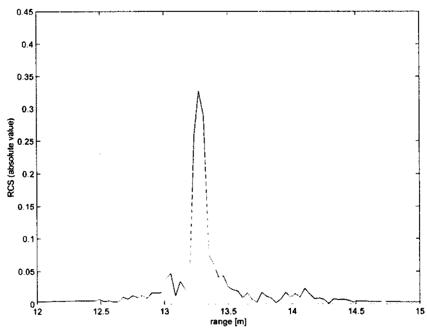

(b) The range profile of target-1 at the aspect angle of 1 deg.

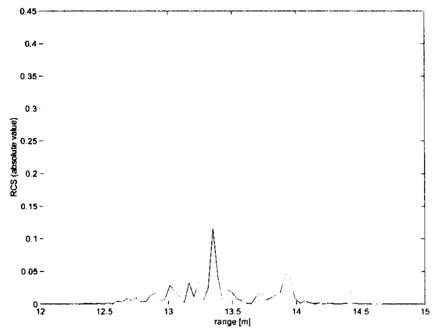

(c) The range profile of target-1 at the aspect angle of 45 deg.

Figure 2. The range profiles of target 1 at some aspect angles.

3. THE CLASSIFICATION WITH SUBCLASS CONCEPT

3.1. Subclass Concept

The range profile is considerably dependent on the aspect angle. Fig. 2 shows the angle dependency of the range profile. Fig. 2(a), (b), and (c) are the range profiles of the Target-1 in Fig. 3, which are obtained by IFFT processing from the data measured at the aspect angles of 0°, 1°, and 45°, respectively. From these figures, we observe that the range profiles vary with the aspect angles, and that they vary in proportion to changes in the aspect angle. Therefore, if we extract feature vectors from the range profiles, the feature vectors are distributed in a highly scattered manner in feature space. Because of range profiles varying

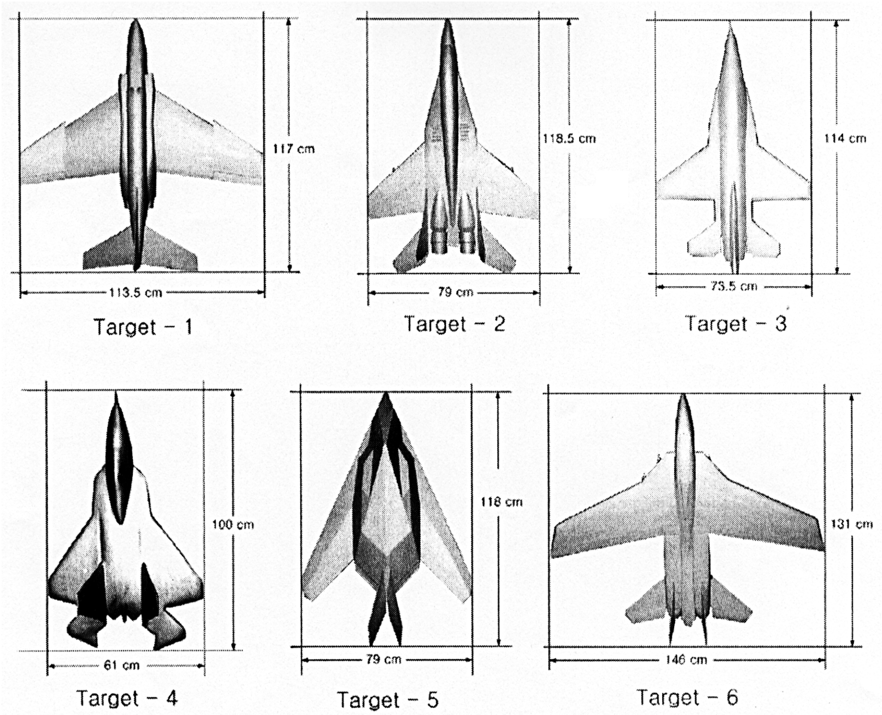

Figure 3. Six aircraft models.

with the aspect angles, the feature vectors extracted from the range profiles have a scattered distribution and occupy a large space in feature space, although they originated from only one class (target). Consequently, the mixed regions, which are mixed by several classes, are extended, and the classification problem becomes more difficult. A conventional statistical classifier, such as the Bayes classifier, does not have discrimination power enough to solve this complex classification problem.

Fig. 4 shows the classification performance of a simple (unimodal) Bayes classifier with respect to the observation angle using measured data from six aircraft models in Fig. 3. The measured data was obtained over the frequency range from 8.3 to 12.3 GHz with a 0.01 GHz step. Across the azimuth aspect, an increment of 0.5° are used for the measurements with the fixed elevation angle of 0 degree. The HH (horizontally transmitting and receiving) polarization were used for the measurement. In this experiment, we select the ratio of training set size versus test set size at about 1:1. In addition, we estimate the

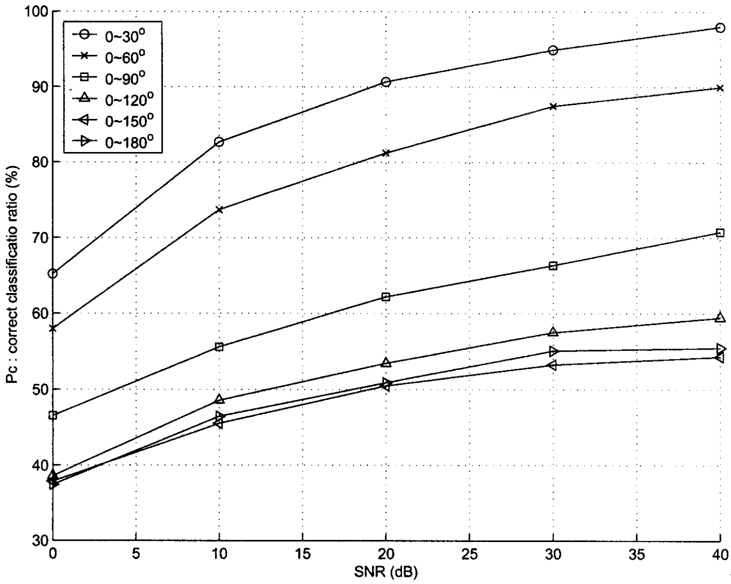

Figure 4. Variation of classification performance via variant angular region.

range profile using inverse fast Fourier transform (IFFT). From this figure, it is easily seen that the classification performance is degraded as the observation angle becomes wider, and the classification result is at most 55% in the case that the observation angle region is from 0° to 180°. These results mean that a conventional statistical classification scheme is not appropriate for the wide-angle target recognition using the range profile.

In order to settle this problem using only a conventional statistical classifier such as a Bayes classifier, we propose a scheme to divide the feature space region taken by each class into more detailed sub-regions. This is the basic idea of the subclass concept in Fig. 1. The detailed sub-regions of one class enable us to model the statistical distribution of its feature vectors in a more efficient manner, rather than only one global region of the conventional Bayes classifier. As a result, the mixed region in the feature space covered by several target classes can be easily identified, resulting in an improvement of target recognition accuracy.

Fig. 5 shows the feature vector distribution of the Target-4 in Fig. 3. For the sake of convenience, we choose only the first and second dimensions of each feature vector extracted from the measured data. In

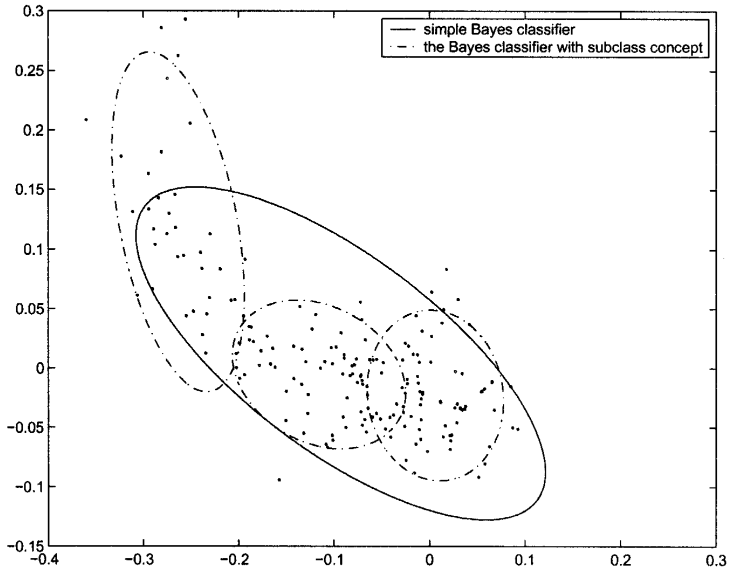

Figure 5. The results of probability density modellings of the simple Bayes classifier and the classifier with a subclasses concept.

Fig. 5, each ellipse represents the trajectory with an equal probability of the conventional Bayes classifier (solid-line) and that of the Bayes classifier with subclass concept (dotted-solid line) consisting of three subclasses, when the associated feature vectors are assumed to obey a normal distribution. That is, all points on each ellipse have the same Mahalanobis distance from each mean of each class [7]. To determine each trajectory, we computed the sample mean vectors and sample covariance matrices from the associated feature vectors.

As shown in Fig. 5, the ellipse of the conventional Bayes classifier can cover some of the feature vectors, but it cannot model most of the feature vectors in the upper-left corner. However, three ellipses associated with the proposed method are capable of modeling most of the feature vectors. In particular, the ellipse of the subclass concept in the upper-left corner can cover the feature vectors that cannot be modeled with that of the conventional Bayes classifier. Therefore, these locally tuned subclasses can improve the discrimination power, because the representation power for each target class is increased, as shown in this figure.

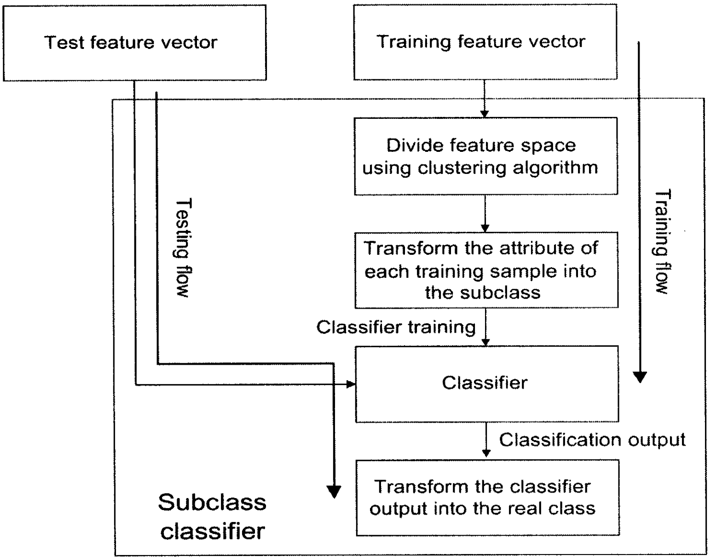

Figure 6. The classifier with subclass concept.

3.2. The Classifier with a Subclass Concept

The classifier with the subclass concept has a training flow and a testing flow, as shown in Fig. 6. However, as represented in this figure, the classifier with the subclass concept has the training flow and testing flow slightly different from the flows of the usual classifier. This is because the probability density functions contained in the proposed classifier are trained not by real classes but by subclasses in the training flow. Also, the testing flow has an additional stage to transform the subclass index (obtained from trained classifier) into the real class index.

The training flow consists of three steps. First, we classify the feature vectors for a class in the training database into several groups using a clustering algorithm. In this paper, we use the fuzzy c-means (FCM) clustering algorithm which uses a fuzzy membership function for clustering [8]. By FCM, the feature vectors are grouped by their distribution in feature space. After grouping, the new class indices for each group are assigned to all of the training feature vectors, and these new class indices are the subclass indices. Next, the classifier is trained using feature vectors in the training data set and the new class indices (the subclass indices).

If the training flow is ended, we can apply the classifier to the test data. This flow follows the testing flow. In the testing flow, we apply the test feature vector to the trained classifier. The output of this classifier is the index for a subclass. However, we do not need the subclass index but the actual class index. Therefore, after the classifier output is decided, we transform the output into the index for a real class. This transformed index is the final result of the classifier with the subclass concept.

4. THE SELECTION OF THE NUMBER OF SUBCLASSES

When applying the classifier with the subclass concept, we must decide the number of subclasses for each class to use this subclass concept in advance. Since the selection of the number of subclasses can seriously affect classification performance, the number of subclasses must be decided optimally. Therefore, we adopt the integer-coded genetic algorithm (GA) [9] for an optimal decision of the number of subclasses.

The structure of each string (each gene) used in the genetic algorithm is as follows. First, we choose each integer in a string as the number of subclasses for a certain class, and the string length is the number of classes (targets). For example, let the total number of classes be 6. Then the length of a string becomes 6. Let *string*1 be [3 5 1 4 7 6]. According to the *string*1, the first class is divided into 3 subclasses, the second class is divided into 5 subclasses, ..., and the sixth (final) class is divided into 6 subclasses. Next, the fitness function must be decided to find out which string is the more optimal solution. In this paper, we select the classification accuracy as the fitness value. The training set is divided into two sets, the new training set and the validation set. The classifier is trained using the new training set and the number of subclasses contained in a string, then validation set is applied to the trained classifier. Next, we calculate the correct classification rate (P_c) using the following equation:

$$\text{Fitness value} = P_c = \frac{\text{The number of correct classified samples}}{\text{Total number of validation samples}}. \quad (12)$$

The procedure of GA operation is as follows [8]:

Step 1 (Initialization):

(a) Initialize a population with randomly generated integer codes (individuals), and let $k = 1$ where k is the index of generation.

(b) perform the classification using the new training set and validation set, and the number of subclass contained in the individuals (strings).

(c) evaluate the correct classification ratio for each string, i.e. the fitness value using (12).

Step 2 (GA operation):

(a) Select two members with a Roullette-wheel strategy.
(b) Apply the crossover operation with the predefined crossover rate.
(c) Apply the mutation to each newly generated individual with the mutation rate.
(d) Repeat (a) to (c) until enough members are generated to form one generation.
(e) $k \leftarrow k + 1$.

Step 3 (Fitness evaluation):

(a) perform the classification as in Step 1. (b).
(b) evaluate the fitness value (the correct classification ratio).

Step 4 (Termination check): If $k > 100$, stop iterating. Otherwise, go back to Step 2.

The two operations used in the above procedure, the crossover and the mutation, are defined as follows:

1) crossover

$$\begin{array}{c} 1\ 2\ 7\ \underline{5}\ 3\ 9 \\ 3\ 3\ 9\ \underline{8}\ 2\ 7 \end{array} \Rightarrow \begin{array}{c} 1\ 2\ 7\ \underline{8}\ 3\ 9 \\ 3\ 3\ 9\ \underline{5}\ 2\ 7 \end{array}$$

2) mutation

$$1\ 2\ \underline{7}\ 8\ 3\ 9 \Rightarrow 1\ 2\ \underline{7+n}\ 8\ 3\ 9$$

where n is the randomly generated integer between 1 and the predefined maximum value of subclasses, K. If the bit changed by mutation exceeds K, we can choose the value by ((the changed value) — K).

5. EXPERIMENTAL RESULTS

In order to investigate the performances of the proposed technique, we measured the RCS of six aircraft models in Fig. 3, at the POSTECH compact range facility. The frequency band of the measurement ranges from 8.3 to 12.3 GHz with a 0.01 GHz step, yielding 401 frequency samples, and aspect angle in the azimuth plane ranges from 0° to 180° with respect to the target's head using a 0.5° increment, resulting in 361 aspects for each target. Note that since the target has a symmetric structure, the feature vectors from the aspect range of 180° $\sim$ 360° are

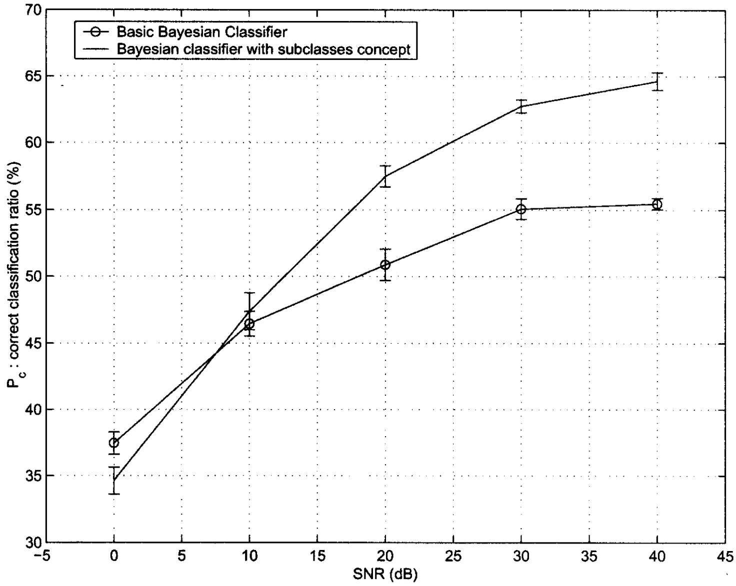

Figure 7. Performance comparison of a simple Bayes classifier and the classifier with a subclass concept (IFFT case).

similar to those of the aspect range of $0° \sim 180°$. The elevation angle of each target is fixed at 0 degree. The HH (horizontally transmitting and receiving) polarization were used for the measurements. In addition, to evaluate the performance in a noisy environment, the measured data was contaminated by additive white Gaussian noise (AWGN) to achieve the desired SNR.

Before the target recognition experiments, we divided the data set into a training set and a test set. We chose uniform angle sampling with an increment of 1° for the training set, and the remaining data sets are selected for the test set. Therefore, we have 181 aspects of each target for the training set, and 180 aspects for the test set. Hence the training set size is about 50% ($181/361 \approx 50\%$) of the overall data set, resulting in about 50% ($180/361 \approx 50\%$) for test set as well. Consequently, the ratio of training data and test data is approximately 1:1.

In Fig. 7, the classification performances were plotted for the simple Bayes classifier (unimodal Bayes classifier with a Gaussian density function) and the Bayes classifier with the subclasses concept using the IFFT range profile and full measured-angular region ($0° \sim 180°$). After the GA operation was performed to decide the number of subclasses, we chose the numbers of subclasses for each class as [6 4 4

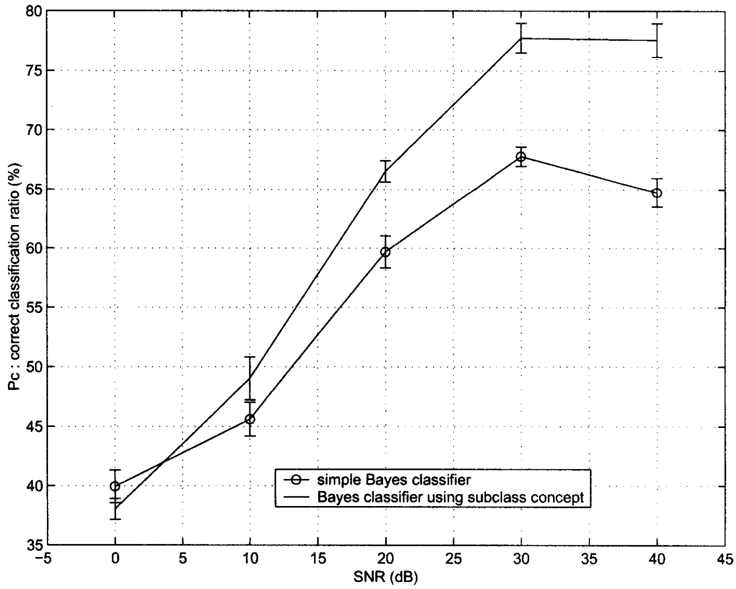

Figure 8. Performance comparison of a simple Bayes classifier and the classifier with a subclass concept (MUSIC case).

7 5 6] with the highest fitness value. The horizontal axis denotes the SNR from 0 dB to 40 dB with 10 dB increments, and the vertical axis denotes the classification performance, i.e., the correct classification rate P_c which is given by

$$P_c = \frac{\text{The Number of correct classified samples}}{\text{Total Number of test samples}} \tag{13}$$

In this figure, we can determine that the accuracy of the classifier with the subclasses concept is better than that of the simple unimodal Bayes classifier, except for the case of $SNR = 0\,\mathrm{dB}$. The reason is that, since noise variance is quite large in 0 dB, the feature vectors may be more scattered by noise and the subclasses may be trained by the distribution of this scattered noise. As the SNR becomes higher, the performance improvement of the proposed classifier is larger, resulting in a 10% improvement at the $SNR = 40\,\mathrm{dB}$.

In Fig. 8, we observed the classification performance in the case of range profile using the MUSIC algorithm, which is capable of generating a high-resolution range profile [5]. In this experiment, we chose the numbers of subclasses of each class as [5 3 2 5 4 3], according to the results of the GA operation. It is noted that the numbers of

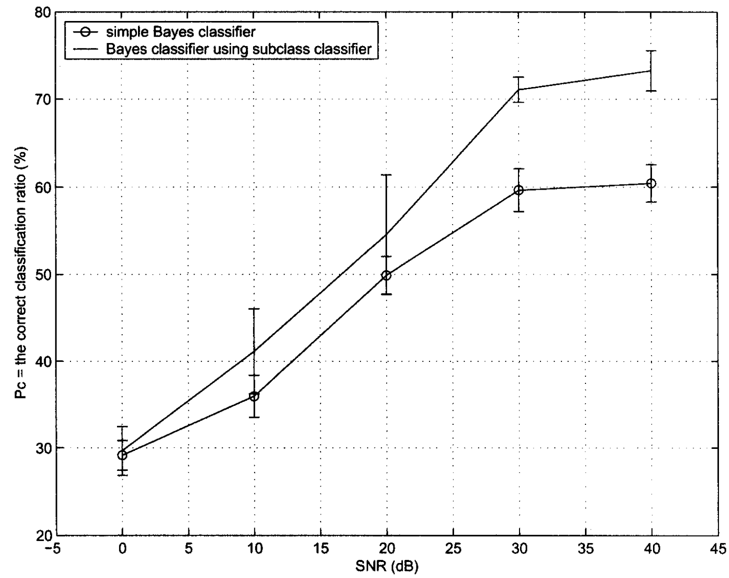

Figure 9. Performance comparison of a simple Bayes classifier and the classifier with a subclass concept (ESPRIT case).

subclasses in this case were slightly smaller than those in the IFFT case. The performance of the proposed classifier was also better than that of the basic Bayes classifier in this figure, except in the low SNR case (0 dB), and ascends to the correct classification of 78% at the high SNR (30 dB $\sim$ 40 dB). In addition, compared to Fig. 7, the results combined with the MUSIC algorithm show much better results than those combined with the IFFT technique. From these results, we conclude that the high-resolution technique is more appropriate in radar target classification over a wide-angular region.

Finally, we investigated the performance of the proposed classifier when combined with 1-D scattering centers on a target rather than range profiles. To estimate 1-D scattering centers on a target, we used the total least squares — estimation of signal parameters via rotational invariance techniques (TLS-ESPRIT). Note that the estimation accuracy of the TLS-ESPRIT is similar to that of the generalized eigenvalues utilizing signal subspace eigenvectors (GEESE) algorithm, which was developed to reduce the computational complexity of the TLS-ESPRIT. In [2], it was shown that, among the various parametric spectral estimators, the GEESE algorithm yielded the most reliable performance in view of target recognition. To carry out the experiment using 1-D scattering centers, we choose the number of subclasses as

[3 6 3 3 3 2], as a result of the GA optimization. Fig. 9 shows that the proposed classifier using the subclass concept can provide more reliable performances than the simple Bayes classifier, even when coupled with the 1-D scattering centers. Furthermore, it is interesting to note that the performance of the proposed classifier with the 1-D scattering centers from the TLS-ESPRIT is superior to that with the IFFT range profiles, especially for high SNR ranges ($30 \sim 40$ dB). However, as the SNR decreases, the IFFT range profiles outperform the 1-D scattering centers estimated by the TLS-ESPRIT. This is because the TLS-ESPRIT is more sensitive to noise than the IFFT range profiles.

6. CONCLUSION

In this paper, we proposed a new classification scheme using 1-D radar signature such as range profiles and scattering centers, in order to prevent the performance degradation of the conventional classifier over a wide angular region. The proposed classifier is based on the subclass concept, which divides a real target class into several subclasses. The feature vectors extracted from the 1-D radar signatures for each target are grouped via a clustering algorithm. Therefore, each group corresponds to each subclass within a target class. The optimum number of subclasses for each target is estimated by a GA operation. Then the Bayes classifier is trained with those subclasses determined by the proposed scheme.

In order to analyze the performance of the proposed classifier, some classification experiments have been carried out. The performance of the proposed classification scheme was shown to have a superior performance over the conventional classification scheme; namely, the unimodal Bayes classifier with a single Gaussian density function. The results imply that our proposed method can improve target recognition capability using range profiles and scattering centers, especially when the angular region is wide, and SNR is larger than about 10 dB.

ACKNOWLEDGMENT

This work was supported in part by the Korean Agency for Defense Development under Contract EM-44, and by the Korean Ministry of Education through its BK21 program.

REFERENCES

1. Kim, K.-T., D.-K. Seo, and H.-T. Kim, "Efficient radar target recognition using the MUSIC algorithm and invariant features," *IEEE Trans. on Antennas and Propagation*, Vol. 50, No. 3, 325–337, Mar. 2002.
2. Kim, K.-T., D.-K. Seo, and H.-T. Kim, "Radar target identification using one-dimensional scattering centres," *IEE Proc. — Radar, Sonar and Navigation*, Vol. 148, No. 5, 285–296, Oct. 2001.
3. Li, H.-J. and S.-H. Yang, "Using range profiles as feature vectors to identify aerospace objects," *IEEE Trans. on Antennas and Propagation*, Vol. 41, No. 3, Mar. 1993.
4. Rosenbach, K. and J. Schiller, "Non cooperative air target identification using radar imagery: Identification rate as a function of signal bandwidth," *IEEE International Radar Conference*, 305–309, 2000.
5. Schmidt, R. O., "Multiple emitter location and signal parameter estimation," *IEEE Trans. on Antennas and Propagation*, Vol. 34, 276–280, Mar. 1986.
6. Haykin, S., *Neural Networks — A comprehensive foundation*, Prentice Hall, Upper Saddle River, New Jersey, 1999.
7. Duda, R. O., P. E. Hart, and D. G. Stork, *Pattern Classification*, John Wiley & Sons, U.S.A., 2001.
8. Jang, J.-S. R., C.-T. Sun, and E. Mizutani, *Neuro-Fuzzy and Soft Computing*, Prentice Hall, Upper Saddle River, 1997.
9. Yokota, T. and M. Gen, "Solving for nonlinear integer programming problem using genetic algorithm and its application," *IEEE International Conference on Systems, Man, and Cybernetics*, Vol. 2, 1602–1609, 1994.
10. Hu, R. and Z. Zhu, "Research on radar target classification based on high resolution range profiles," *Aerospace and Electronics Conference, NAECON 1997, Proceedings of the IEEE 1997 National*, Volume 2, 951–955, 1997.
11. Roy, R. and T. Kailath, "ESPRIT — Estimation of signal parameters via rotational invariance techniques," *IEEE Trans. on Acoustics, Speech, and Signal Processing*, Vol. 37, No. 7, 984–995, July 1989.